

N O T I C E

THIS DOCUMENT HAS BEEN REPRODUCED FROM
MICROFICHE. ALTHOUGH IT IS RECOGNIZED THAT
CERTAIN PORTIONS ARE ILLEGIBLE, IT IS BEING RELEASED
IN THE INTEREST OF MAKING AVAILABLE AS MUCH
INFORMATION AS POSSIBLE

(NASA-TM-83868) SOME NEW METHODS IN
GEOMAGNETIC FIELD MODELING APPLIED TO THE
1960 - 1980 EPOCH (NASA) 42 P HC A03/MF A01
CSCI 08N

N82-17714

Unclas

G3/46 11741

NASA

Technical Memorandum 83868

**Some New Methods in
Geomagnetic Field Modeling
Applied to the 1960 - 1980 Epoch**

R. A. Langel, R. H. Estes and G. D. Mead

DECEMBER 1981

National Aeronautics and
Space Administration

Goddard Space Flight Center
Greenbelt, Maryland 20771



SOME NEW METHODS IN GEOMAGNETIC FIELD MODELING
APPLIED TO THE 1960-1980 EPOCH

R. A. Langel¹
K. H. Estes²
G. D. Mead¹

¹ NASA/Goddard Space Flight Center, Greenbelt, Maryland 20771

² Business and Technological Systems, Seabrook, Maryland 20801

Accepted for publication in the Journal Of Geomagnetism and Geoelectricity

INTRODUCTION

As shown by Gauss in 1839 the potential of the geomagnetic field can be represented by a spherical harmonic series of the form:

$$V = a \sum_{n=1}^{NMAX1} \sum_{m=0}^n \left(\frac{a}{r}\right)^{n+1} [g_n^m \cos m\phi + h_n^m \sin m\phi] P_n^m(\cos \theta) \\ + a \sum_{n=1}^{NMAX2} \sum_{m=0}^n \left(\frac{r}{a}\right)^n [q_n^m \cos m\phi + s_n^m \sin m\phi] P_n^m(\cos \theta) \quad (1)$$

where: a is the mean radius of the earth,

r, θ, ϕ are the standard spherical coordinates, and

P_n^m (in "modern" methodology) are the Schmidt quasi-normalized form of associated Legendre functions.

The magnetic field is then given by:

$$\vec{B} = -\nabla V = (B_r, B_\theta, B_\phi). \quad (2)$$

Theoretically, (1) applies exactly, at a given time, only when NMAX1 and NMAX2 go to infinity, under the assumption that the region under consideration, $a < r < b$, say, is source-free. The source-free assumption holds nearly exactly between the earth's surface and the ionosphere, but near-earth spacecraft pass through a region of "field aligned" currents in the auroral belt. The geometry is such that the field magnitude and vertical component are relatively unaffected (Langel, 1974) but the horizontal components may have several hundred nT (nanotesla) contribution from these currents. This must be accounted for in deriving (1). In practice, the values of NMAX1 and NMAX2 are limited by the data accuracy, by finite computer capabilities and, for NMAX2, the nature of its temporal variability. The data accuracy aspect will be

discussed in a later section. In (1) the terms in $(a/r)^{n+1}$ describe sources within $r < a$, or "internal" sources, and the terms in $(r/a)^n$ describe sources outside $r \geq a$, or "external" sources. Field measurements are used to derive the coefficients g_n^m , h_n^m , q_n^m , and s_n^m , usually by some form of least squares procedure.

Both the internal (g_n^m and h_n^m) and external (q_n^m and s_n^m) coefficients are known to vary with time. To date, temporal variations in the external terms have not been included in models. Variations in the internal field have been modeled by expanding the coefficients in Taylor series in time, e.g.:

$$g_n^m(t) = g_n^m(t_0) + \dot{g}_n^m(t_0)(t-t_0) + \ddot{g}_n^m(t_0) \frac{(t-t_0)^2}{2!} + \dots \quad (3)$$

Most models include only the constant and first derivative (secular variation) terms, although some more recent models have incorporated the second derivative (secular acceleration) also (e.g., Cain et al, 1967; Barraclough and Malin, 1979). It should be noted that in some contexts the derivatives in equation (3) are combined with the factorials to produce the total coefficients which multiply the powers of time in the power series.

The principal sources of data for main field modeling have been (1) permanent magnetic observatories, (2) repeat measurements at selected sites with intervals between measurement of one to six years, (3) surveys from aircraft and ship, and (4) satellite measurements. Only the satellite surveys are truly global. Relevant surveys from which data are generally available were conducted by the Cosmos 49 spacecraft in October and November of 1964, by the OGO-2, -4, and -6 (POGO) spacecraft from October 1965 through July 1971, and most recently, by the MAGSAT

spacecraft from November 1979 through June 1980. The Cosmos and POGO satellites measured only the field magnitude, which introduces an ambiguity in resulting spherical harmonic analyses (Backus, 1970; Hurwitz and Knapp, 1974; Stern and Bredekamp, 1975; Stern et al, 1980). The permanent magnetic observatories must still be regarded as the primary source of information regarding the temporal changes. Unfortunately, these data, and all data except the satellite data, are highly "contaminated" by fields originating in the crust of the earth. These anomaly fields can be tens to thousands of nT in any of the components and represent a large noise source when attempting to model the bulk of the geomagnetic field which originates in the earth's core.

This paper describes an attempt to utilize the observatory data in a more optimal way by incorporating an estimation of individual observatory anomaly fields into the solution and, in so doing, to allow the derivation of a more accurate model of temporal variation. The results were presented as a possible contribution to the 1980 version of the IGRF (International Geomagnetic Reference Field) and the definitive Geomagnetic Reference Fields for 1965, 1970 and 1975 at the 1981 assembly of the International Association of Geomagnetism and Aeronomy (IAGA).

MODEL DEGREE AND ORDER

In (1) "n" is the degree and "m" the order of any given term. NMAX1 is the maximum degree and order for internal terms and NMAX2 for external terms. Gauss' original model did not include external terms and used an NMAX1 of four because he concluded that the available data did not warrant the inclusion of further terms. In the years since Gauss the available data base has improved considerably and, accordingly, the degree/order of published models has increased. Malin and Pocock (1969) analyzed the question of the appropriate degree/order for models based on magnetic observatory data. Using data from 180 observatories they computed models from degree/order two to ten and compared the rms residuals. Their results are shown in Table 1.

TABLE 1

Degree/Order	rms residual (nT)
2	3495.7
3	2218.2
4	889.0
5	538.7
6	388.5
7	364.5
8	359.5
9	354.3
10	351.9

They note a rapidly decreasing rms from 2nd to 6th order after which the decrease becomes very slow; this leveling off is attributed to the "crustal noise" in the data. They conclude that "at least six orders should be evaluated if the core field is to be fitted within 0.5 per cent". Subsequent models not using satellite data are in reasonable agreement with their results and most of these models were of degree/order eight, nine or ten.

The situation changed drastically with the advent of satellite data, particularly the surveys by the POGO satellites from 1965 to 1971. These data are far enough above the earth that the crustal anomaly fields are less than 20 nT maximum, with rms below 5 nT. Further, the coverage is now truly global with no large gaps. The latest published models which include these data are mainly of degree/order 12 (Rarraclough et al, 1975; Peddie and Fabiano, 1976; Barker et al, 1981). Those of us who have been attempting to study crustal magnetic anomalies have been using a model of degree/order 13 (Langel et al, 1980a). This choice is confirmed by Langel and Estes (1982) who derived the spatial power spectrum: (Loves, 1966, 1974),

$$R_n = (n+1) \sum_{m=0}^n [(g_n^m)^2 + (h_n^m)^2] \quad (4)$$

for $n=1$ to 23 using Magsat data. The derived spectrum showed a clear break near $n=14$ which was interpreted to mean that the core field dominates for $n < 13$ and the crustal field for $n > 15$.

The situation for the temporal derivative terms is much more complicated. In the model to be presented, we have included first derivatives to degree/order thirteen, second derivatives to degree/order six, and third derivatives to degree/order four. For each coefficient we have calculated the ratio of coefficient magnitude to the standard error of the coefficient. As a rule of thumb, we assume that if this ratio is ≥ 2 , the coefficient has statistical significance above the 95% confidence level (see, e.g. Barraclough and Malin, 1979).

Table 2 shows the ratio distribution for these terms. On this basis we are justified in including some terms from each of the 13 degrees of the first derivative and, perhaps, should have extended the second and third derivative terms to still higher degree/order. Investigation of this question is beyond the scope of the present paper.

Aside from the question of the accuracy to which individual coefficients are determined, one has to ask what the descriptive and predictive properties are for models with higher derivatives. We will address this question in a subsequent section.

There remains the question of external fields (NMAX2). As Malin and Pocock (1969 and references therein) point out, various attempts have been made to separate the internal and external parts of the field. However, the results have been widely different; in some cases unrealistically large external fields have been found, but have not been statistically significant. Again, a change has come with the global vector survey by MAGSAT. Langel et al (1980b) used data from November 5-6, 1979 to derive the MGST(6/80) model. This model included statistically significant external terms of degree/order equal to one. Furthermore, plots of the MAGSAT data clearly demonstrated the need for such terms to adequately represent the data. However, it is known that

Table 2:
Summary of Distribution of Ratio of Coefficient
Magnitude to Coefficient Standard Error.

Degree	Number of Terms	R A T I O S			
		>100	10-100	2-10	<2
<u>First Derivatives</u>					
1	3	1	2	0	0
2	5	3	0	2	0
3	7	0	6	1	0
4	9	0	6	3	0
5	11	0	8	3	0
6	13	0	10	3	0
7	15	1	9	4	1
8	17	0	12	4	1
9	19	0	12	6	1
10	21	0	8	8	5
11	23	0	6	15	2
12	25	0	2	17	6
13	27	0	4	11	12
<u>Second Derivatives</u>					
1	3	0	3	0	0
2	5	0	1	4	0
3	7	0	6	1	0
4	9	0	5	3	1
5	11	0	7	3	1
6	13	0	12	0	1
<u>Third Derivatives</u>					
1	3	0	3	0	0
2	5	1	3	1	0
3	7	0	7	0	0
4	9	0	5	3	1

the sources of the external fields, which are the magnetospheric ring current, magnetopause current and magnetotail current, vary widely with time in a fashion not yet amenable to this type of model and, moreover, vary more strongly as functions of local time than of longitude as set forth in equation (1). While external terms may be valuable as an indication of the average quiet level of external fields, we have no compelling reason to include them in models describing extended periods of time.

METHOD OF ANALYSIS

The method of determining the parameters of (1) is essentially the same as that described by Cain et al (1967) with revisions to include higher temporal derivatives and to incorporate magnetic observatory data in a new way. Because of the data types involved the problem is non-linear and must be solved iteratively. The Bayesian least squares estimation equations are as follows:

$$\delta \hat{p}_{n+1} = (A^T W A + \Omega_0^{-1})^{-1} [A^T W \delta y_n + \Omega_0^{-1} (\hat{p}_0 - \hat{p}_n)] \quad (5)$$

where

- A is the partial derivative matrix of the measurements with respect to the parameters
- \hat{p} is the vector of adjusted parameters
- δy is the vector of residuals, i.e. measured data minus predicted value from previous iteration
- W is the weight matrix for the measurements
- Ω_0 is the *a priori* parameter covariance matrix

$\hat{\rho}_0$ is the *a priori* estimate of the parameters

and the estimate at the (n+1)st iteration is

$$\hat{\rho}_{n+1} = \hat{\rho}_n + \delta\hat{\rho}_{n+1} \quad (6)$$

In the notation of Cain et al (1967), each measured quantity, say C, is a function of the coefficients g_n^m , h_n^m , q_n^m , and s_n^m from equation (1), denoted collectively by "p", and of the standard r, θ, ϕ, t space-time coordinates:

$$C = C(p; r, \theta, \phi, t) \quad (7)$$

The partial derivatives in A are then the set $\partial C / \partial p$. The weight matrix W is diagonal and formed from the standard deviations of the various measurements, so that for the *i*th measurement with sigma σ_i

$$W_{ii} = \frac{1}{\sigma_i^2} \quad (8)$$

As already noted, the data from magnetic observatories represent the most useful data set for determining the temporal variation of the internal field. The incorporation of such data directly into a main internal core field model, however, suffers from the fact that the magnetic field measured at the observatory may have a significant contribution due to local crustal fields. The field at an observatory is represented as the vector sum

$$\vec{B} = \vec{B}_i + \vec{B}_m \quad (9)$$

where \vec{B}_i is the internal core field contribution from the scalar potential of equation (1) and \vec{B}_m is the local anomaly field, which may

change appreciably over a distance of a few kilometers. The time derivative of \bar{B}_m is assumed to be negligible so that

$$\dot{\bar{B}} = \dot{\bar{B}}_1 . \quad (10)$$

A global satellite data set, on the other hand, is comparatively free from the effects of crustal anomalies and is certainly free from the effects of the higher-amplitude, more localized anomalies. Assuming that for a main field model the crustal influence on satellite data may be treated as random noise, these data may then be used in conjunction with observatory data to isolate the non-core fields at the observatory. In terms of the algorithm of equations (5), (7) and (8) this is accomplished by writing, for each measured component at each observatory

$$C = C(p, C_a; r, \theta, \phi, t), \quad (12)$$

where C_a is the anomaly in that component at that observatory. Terms such as $\partial C / \partial C_a$ are then added to the matrix, A , of partial derivatives. The vector, p , of adjusted parameters from equation (5) then includes p and all anomaly components. This procedure allows the data to properly distribute their influence among the temporal and constant parameters in a least square sense. Such a solution is well determined only when the satellite data, not strongly sensitive to the crustal fields, are included in the solution. A forward elimination technique is used for the anomaly components in accumulating the normal matrix A^TWA , so the cost of obtaining the solution for the model coefficients is greatly reduced. The values of the anomaly components, if desired, are then obtained by back substitution.

DATA SET

The data utilized in the present analysis include data from (1) magnetic observatories, (2) repeat stations, (3) marine surveys, (4) the

POGO satellite surveys and (5) the MAGSAT satellite survey. The POGO data consisted of the 47000 scalar observations used for the POGO(8/71) model (Langel, 1974) augmented with 24000 quiet OGO-6 observations from mid-1969 through early 1971. The MAGSAT data set, consisting of scalar and vector measurements from November 5 and 6, 1979, is identical to that used for the MGST(6/80) model (Langel et al, 1980b). The measurement standard deviation used to weight the POGO data was 7 nT and for MAGSAT data was 10 nT, based on fits to these data alone.

Annual means data were taken from 148 observatories, selected on the basis of geographical distribution, longevity of measurement availability, and data quality. This resulted in our not using some high quality observatories in regions of higher observatory density. Moreover, only those annual means with three vector components were accepted. The observatories utilized are listed in Table 3 together with the anomaly vector bias from the solution, the time of data availability and the σ_j used in equation (8). The spellings used are those of the NOAA World-Wide Magnetic Survey of the National Geophysical and Solar-Terrestrial Data Center. In cases where a significant change at the observatory (e.g., shift of location, change of instrument) was known to have occurred, the data from that observatory were broken into subsets which were treated independently with respect to the anomaly bias vectors. In all cases the measured elements were converted to X, Y and Z components where X is north, Y is east and Z is down in a geodetic coordinate system assuming an equatorial radius of 6378.165 km and a reciprocal flattening of 298.25. To determine the σ_j in Table 3 a least squares quadratic curve was fit to each component at each observatory and the standard deviation of the data to the solution adopted as σ_j .

To fill in surface areas void of data, selected marine survey and repeat station data were utilized. In order to accommodate the non-

ORIGINAL PAGE IS
OF POOR QUALITY

Table 3

STATION	LAT	LONG	ANOMALY BIAS			TIME INTERVAL	MEASUREMENT SIGNALS		
			X	Y	Z		X	Y	Z
ADDIS ABABA	9.03	36.76	489.5	15.1	148.6	1960.5-70.5	2.3	3.6	1.0
AGINCOURT	43.78	-74.27	-45.7	175.7	-140.4	1960.5-69.1	8.2	3.9	4.5
ALERT	82.90	-62.30	9.7	34.6	-142.2	1961.9-74.5	12.7	15.9	24.0
ALIBAU	16.64	72.87	-80.2	403.7	669.0	1960.5-73.5	16.3	7.5	9.4
ALMA ATA	42.25	76.92	125.9	42.2	-192.1	1961.5-70.5	5.6	14.0	16.2
ALMERIA	36.85	-2.40	-6.0	8.6	22.2	1960.5-70.5	6.7	6.2	4.3
AMERLEY	-43.15	172.72	-44.0	-16.6	70.1	1960.5-70.5	5.0	4.5	6.6
ANNARALAINAGAP	11.37	79.68	219.5	-60.4	-174.6	1960.5-74.5	11.3	9.5	17.3
APIA	-13.81	-171.76	-86.4	206.1	-1017.2	1960.5-70.5	7.6	6.5	3.7
APUIA	42.38	13.32	-8.4	42.2	9.5	1960.5-70.5	6.2	6.4	5.8
ARGENTINE ISLAND	-63.24	-64.26	69.3	-93.5	512.8	1960.5-67.5	1.4	1.3	2.5
BAHR LAKE	64.33	-93.03	149.0	-1.9	-102.8	1960.5-68.5	2.0	6.5	16.2
	64.33	-96.03	219.4	-104.7	-114.3	1960.5-70.5	8.0	19.1	31.1
BANGUI	4.44	18.50	-85.6	47.0	95.0	1960.5-68.5	5.4	12.7	5.2
	4.44	18.50	-119.3	37.6	107.3	1960.5-74.5	2.2	22.9	1.5
BARROW	71.30	-156.75	23.9	-96.1	-32.0	1960.5-77.5	11.5	6.2	26.6
BELSK	51.84	20.79	96.5	152.5	314.0	1960.5-70.5	4.7	9.0	3.1
BEREZNYAYI	49.82	71.08	-423.6	14.7	338.9	1960.5-70.5	6.9	7.6	13.9
BINZA	-4.27	15.37	-144.4	-118.0	-177.5	1960.5-66.5	6.3	4.2	4.4
BUKHNOYA	74.50	19.20	-107.6	40.7	37.8	1960.5-64.5	0.7	1.6	5.0
	74.50	19.20	-119.9	44.6	2.9	1960.5-69.5	0.8	1.5	2.1
	74.50	19.20	-122.1	47.1	28.0	1970.5-72.5	0.7	1.6	5.3
BOULDER	-60.14	-105.24	-92.5	53.5	-160.3	1960.5-77.5	7.6	3.1	9.0
BYRD	-60.02	-119.52	-24.2	37.5	-147.2	1961.5-68.5	4.0	2.0	7.6
CASTLE NOCA	37.24	-122.13	-128.6	-16.5	5.7	1970.5-74.5	0.9	1.0	3.8
CHA PA	22.35	103.83	-119.6	-90.5	-2.9	1960.5-75.5	21.6	7.4	25.3
CHANDON FORET	46.02	2.26	-79.7	-24.5	114.0	1960.5-75.5	6.1	5.9	3.4
CHMELYSKIN	77.72	104.28	-49.7	-95.0	-80.1	1960.5-70.5	11.1	4.4	21.6
COIMBRA	40.22	-6.42	-5.4	-22.4	48.0	1960.5-70.5	9.9	7.5	8.6
COLLEGE	64.86	-147.64	-17.4	-60.7	-107.3	1960.5-77.5	5.0	6.3	3.4
DALLAS	32.44	-96.75	-15.1	23.6	-73.5	1960.5-74.5	10.6	2.8	3.2
DIKSON	73.55	80.57	-114.5	-140.0	-276.3	1960.5-62.5	9.0	5.2	7.4
	73.55	80.57	-104.5	-147.6	-246.6	1961.5-70.5	9.0	5.2	7.4
DOMBAS	62.07	4.12	-93.7	-79.0	-234.8	1960.5-74.5	5.1	8.2	2.7
DOUMBE	73.10	4.54	-7.7	-16.6	48.4	1960.5-70.5	4.9	8.3	2.4
DUMONT JURVILLE	-66.66	140.01	-172.8	-389.2	-2687.6	1960.5-72.5	14.6	15.7	36.3
	-66.66	140.01	-192.0	-419.3	-2892.9	1973.5-75.5	14.6	15.7	36.3
DUSHETI	-42.09	44.70	-238.4	4.6	-62.7	1960.5-74.5	7.5	3.6	12.9
DYMER	50.72	30.30	-26.6	90.1	117.9	1960.5-70.5	4.0	5.7	3.7
FORT MURCHILL	38.77	-94.10	-140.2	46.8	-255.8	1960.5-70.5	5.4	8.6	9.0
FREDERICKSBURG	38.21	-77.37	28.1	-69.7	120.5	1960.5-77.5	16.4	3.4	19.4
FUJUEME	5.47	-73.74	14.4	-48.7	215.8	1960.5-74.5	2.6	4.0	23.9
FURSTENFELDENHUCK	46.17	11.26	-31.2	-5.4	14.9	1960.5-70.5	5.6	7.8	4.5
GANGARA	-31.78	115.95	-91.0	-127.8	122.5	1960.5-70.5	2.7	5.4	12.7
GODMAYN	69.24	-53.52	207.6	-257.3	669.0	1960.5-73.5	5.2	3.0	9.5
GONNOTAYEZMAYA	43.68	132.17	-13.3	-23.5	-37.8	1960.5-70.5	14.2	7.2	18.2
GRAT SWALE R	55.27	-77.78	258.3	113.5	-54.9	1960.5-75.5	10.0	4.3	14.2
GRUCKA	44.63	20.77	-40.0	-48.9	-51.1	1960.5-70.5	5.6	7.3	6.0
GUAN	13.58	144.67	174.9	104.3	-2.7	1960.5-77.5	9.1	4.4	5.2
HALLEY BAY	-75.52	-26.68	-26.3	400.2	-7.4	1960.5-66.5	8.3	11.3	35.1
HARTLAND	51.00	-4.48	-54.6	7.0	64.2	1960.5-70.5	5.2	8.8	5.0
HCL	54.61	18.61	31.6	-157.2	-73.6	1960.5-68.5	1.3	2.1	5.2
HERRANUS	-34.42	14.22	-17.6	24.0	-5.7	1960.5-75.5	8.6	2.9	3.1
HONJULMU	21.32	-156.00	-174.4	112.9	-304.6	1961.5-77.5	6.2	2.2	4.1
HUANCAYU	-12.04	-75.34	90.3	46.5	246.8	1960.5-70.5	11.0	3.1	16.0
HYERABAD	17.41	78.55	352.2	109.6	457.0	1960.5-70.5	6.1	22.3	15.8
ISTANOL KNJILLI	41.06	29.06	171.5	121.7	1.9	1960.5-75.5	5.9	7.8	7.7
KAKIDRA	36.23	140.19	-1.5	0.5	-69.8	1960.5-64.5	2.1	0.3	0.9
	36.23	140.19	-6.6	3.1	-64.3	1960.5-70.5	7.6	3.5	3.4
KELES	41.42	69.20	-219.5	-43.4	-12.4	1960.5-63.5	0.6	0.3	0.7
KERGULEN	-49.35	70.20	177.2	206.1	633.0	1960.5-75.5	5.4	11.8	25.7
KIEV	50.72	70.30	-70.4	167.7	129.9	1960.5-63.5	0.1	1.4	1.5
KLYUCHI	55.03	81.90	159.1	-68.2	6.3	1967.5-70.5	4.3	1.4	4.7
KRASNAYA PAKHRA	55.46	37.31	108.3	-12.8	243.5	1960.5-70.5	4.6	9.4	7.4
KSARA	33.82	35.69	-67.1	67.4	-77.7	1960.5-70.5	4.8	2.9	36.2
LEIVOGUR	64.18	-21.70	-209.9	504.9	-482.9	1960.5-75.5	6.4	10.8	11.9
LERNICK	66.13	-1.16	-137.3	169.3	37.7	1960.5-70.5	4.7	11.4	4.7
LOGRONO	42.46	-2.51	-2.3	0.6	50.4	1960.5-70.5	6.8	7.1	3.4
LOPASKOYE	66.25	33.68	96.1	337.4	-411.6	1961.5-70.5	5.6	9.5	6.7
LORENCO MARGES	-25.92	32.56	128.5	34.2	-159.6	1960.5-71.5	6.4	3.8	7.7
LOVO	59.35	17.61	35.2	0.9	7.5	1960.5-70.5	5.1	4.6	3.7
LUANDA DELAS	-6.92	13.17	193.6	-6.4	50.0	1960.5-74.5	7.6	4.0	18.2
LUMPING	25.00	121.17	16.0	-34.6	79.9	1960.5-74.5	4.3	22.5	5.4
LYOV	49.90	23.75	128.9	125.3	153.7	1960.5-70.5	7.3	9.6	9.0
LUIRO	-2.25	28.60	246.5	130.7	19.6	1960.5-70.5	7.5	2.3	2.5
M BANE	14.39	-16.96	143.0	-48.4	78.8	1960.5-71.5	7.5	3.6	4.3
MACNAMIE ISLAND	-44.50	156.45	236.3	-7.3	309.5	1960.5-70.5	4.4	5.6	6.0
MAGARAN	66.12	151.02	-136.2	346.4	1273.7	1960.5-66.5	1.6	1.1	30.4
MAURITIUS	-20.09	57.55	475.5	-201.6	-441.5	1960.5-65.5	5.7	3.6	12.2
MAUSON	-67.60	62.68	16.7	25.0	197.7	1960.5-70.5	7.3	9.5	25.3
MEANOOK	54.62	-113.33	67.9	6.3	-160.3	1960.5-75.5	6.5	12.1	11.5
MEANGETSU	43.91	144.14	-239.3	133.1	77.2	1960.5-70.5	10.4	4.2	8.6
MIBNY	-66.55	93.02	-139.1	50.2	-428.5	1960.5-70.5	5.5	5.8	20.2
MISALLAT	29.52	36.69	-90.1	73.6	123.4	1960.6-73.5	7.4	4.5	4.8

ORIGINAL PAGE IS
OF POOR QUALITY

Table 3 (Cont'd)

STATION	LAT	LONG	ANOMALY BIAS			TIME INTERVAL	MEASUREMENT SIGMAS		
			X	Y	Z		X	Y	Z
NBCA	3.34	8.04	-102.0	1.4	151.0	1900.5-71.5	0.0	0.0	1.0
NELADZHMAYA	-07.07	49.45	-40.0	-95.5	-207.4	1905.5-70.5	11.9	7.3	91.0
NEMAL BAY	70.20	-119.40	-22.4	5.0	-40.7	1902.0-70.5	5.1	11.7	9.3
NMINTILUPA	14.38	121.02	-04.2	-103.0	19.1	1900.5-75.5	12.7	0.2	9.0
NAIBBI	-1.33	30.81	47.4	02.0	-40.1	1904.5-70.5	7.4	3.7	10.9
NAISSARSUAU	01.10	-49.20	-173.2	273.1	579.5	1900.5-73.5	10.4	5.5	11.5
N'PORT	40.20	-117.12	-71.3	110.2	-129.2	1900.0-77.5	3.0	4.1	3.0
NIBNEK	52.07	12.07	-41.3	0.1	-60.0	1900.5-75.5	5.3	0.2	2.9
NOVOLAZAREVSKAY	-70.77	11.03	-310.9	72.4	194.0	1901.5-70.5	0.1	9.4	40.5
NOVRIJARVI	00.51	24.05	271.1	-98.3	107.2	1900.5-75.5	5.0	9.0	4.3
NYTANA	45.40	-75.55	104.7	-143.0	104.7	1904.7-74.5	2.0	2.7	3.0
PANAGYURISHTE	42.52	24.10	-197.1	-107.7	-102.1	1900.5-75.5	0.0	5.4	10.5
PARAMANBO	5.01	-95.22	-25.1	-32.2	-1.5	1900.5-74.5	7.9	0.2	10.2
PARATUNKA	52.00	150.43	-350.5	225.1	271.0	1900.5-70.5	1.0	2.9	1.5
PATONY	52.17	104.45	0.0	40.0	-79.2	1900.5-70.5	11.7	5.7	19.0
PILAR	-31.07	-63.03	77.2	-10.0	42.3	1900.0-74.5	11.7	12.0	5.4
PLAISANCE	-20.43	57.07	0.0	0.0	790.0	1900.5-70.5	90.0	90.0	0.9
PLESMENITZI	54.50	27.00	204.9	100.4	-104.9	1902.5-07.5	2.0	1.3	3.0
	54.50	27.00	204.9	148.3	-119.0	1900.5-70.5	2.0	1.0	2.2
POKLAN TUNGUSKA	61.00	90.00	20.9	54.2	-293.3	1909.5-75.5	2.9	2.1	3.9
PORT MOKRESKY	-9.41	147.15	-40.2	59.0	103.4	1900.5-75.5	4.4	5.7	9.1
PRUNOVICE	49.99	14.55	-51.4	25.4	-09.2	1900.5-71.5	4.0	2.0	0.2
QUETTA	30.19	00.95	-3.0	52.0	-30.4	1900.5-07.5	3.0	2.9	3.4
	30.19	00.95	-11.3	50.7	-54.0	1900.5-75.5	2.0	13.3	17.9
QUIACA	-22.10	-05.01	88.5	-54.4	100.9	1900.5-74.5	13.1	15.4	4.0
RESOLUTE BAY	74.70	-94.90	30.7	30.1	72.0	1900.5-75.5	10.4	7.2	8.2
ROBURENT	44.30	7.09	70.5	40.0	117.7	1904.0-05.5	5.2	3.3	0.9
	44.30	7.09	00.0	-50.3	143.9	1900.5-08.5	5.2	3.3	0.9
	44.30	7.09	81.3	59.1	89.1	1900.5-73.5	5.2	3.3	0.9
RUDE SKOV	55.04	12.40	19.1	-5.5	-33.4	1900.5-70.5	5.3	9.3	3.4
SABNAMALA	30.30	77.00	-15.2	-27.0	03.0	1904.5-73.5	4.0	7.1	13.0
SAN JUAN	10.30	-00.12	01.0	33.5	220.0	1900.5-04.5	1.2	0.9	2.7
	10.12	-00.15	-139.3	102.0	213.0	1905.5-77.5	0.0	2.0	15.0
SAN MIGUEL	37.77	-25.05	004.7	421.2	1711.4	1900.5-70.5	10.7	30.8	11.1
SANAE	-70.30	-2.37	-51.4	-19.1	20.0	1902.7-70.5	4.2	3.9	5.5
	-70.30	-2.37	-00.7	-72.7	-5.0	1971.7-75.5	0.4	1.2	0.7
SCOTT BASE	-77.05	100.70	-2270.1	-930.0	-3700.9	1900.0-70.5	7.9	7.9	11.2
SIMOSATO	33.50	135.94	-40.0	29.4	20.9	1900.5-75.5	15.7	3.7	5.0
SITKA	57.00	-135.33	-11.0	-14.5	-02.9	1900.5-77.5	5.0	0.9	4.0
SODANKYLA	07.37	20.03	-104.0	-104.3	-570.9	1900.5-75.5	4.7	10.5	3.4
SOUTH POLE	-09.99	-13.32	-1342.7	-3009.0	79.0	1900.5-71.5	0.7	7.2	22.5
ST JOHN S	47.59	-52.00	9.0	20.5	-2.1	1900.0-70.5	1.7	3.0	4.1
STENOLINIY	00.12	151.02	-209.9	-742.5	52.5	1900.5-70.5	2.0	1.7	0.0
STEPANOVKA	40.70	30.00	-123.1	-000.5	00.1	1900.5-70.5	4.0	7.0	0.9
SYDRA BASE	-09.01	39.59	-24.3	-02.9	-14.7	1900.0-00.5	0.1	10.4	10.5
TANITI	-17.57	-149.50	-075.0	-091.5	-209.7	1900.2-72.5	7.1	2.0	4.1
	-17.57	-149.50	-075.0	-091.5	-209.7	1973.5-73.5	7.1	2.0	4.1
TARANASSET	22.79	5.53	120.4	-200.0	-70.0	1900.5-70.5	2.9	1.3	1.1
TANANARIVE	-10.92	47.50	371.9	0.2	-447.3	1900.5-74.5	0.4	0.3	12.7
TATUCCA	-1.20	-40.51	31.4	-177.5	09.7	1900.5-71.5	0.9	4.5	12.0
TEHRAN	35.74	51.30	-114.1	13.9	-192.2	1900.5-70.5	0.7	3.0	13.4
TENRIFE	20.40	-10.20	-70.4	07.5	-1051.2	1900.5-75.5	13.4	7.9	75.0
TEOLOYUCAN	19.75	-99.10	-124.0	3.0	-11.9	1900.5-70.5	0.0	10.9	14.2
	19.75	-99.10	-07.0	30.1	-40.7	1971.5-75.5	23.2	0.5	3.0
THULE II	77.40	-09.17	-95.9	104.9	13.3	1900.5-73.5	0.3	1.5	5.4
TIMANY	40.90	17.09	-10.0	-10.0	-27.7	1900.5-70.5	7.3	0.2	5.2
TIKSI	71.50	129.00	-112.2	-159.0	-134.0	1900.5-07.5	3.0	2.9	13.3
	71.50	129.00	-00.1	-104.1	-00.0	1970.5-70.5	4.3	0.9	0.7
TORSK	50.47	04.93	-21.7	-04.5	-239.8	1900.5-09.5	5.9	2.1	4.0
TOOLANGI	-37.53	149.47	-40.9	-22.0	42.0	1900.5-70.5	4.0	0.3	4.2
TRELEN	-43.25	-05.32	170.9	5.0	25.0	1900.5-70.5	4.0	3.5	3.4
TRIVANDRUM	0.40	70.95	215.3	99.0	79.5	1900.5-04.5	5.1	0.7	3.1
	0.40	70.95	255.0	195.2	73.0	1905.5-74.5	4.3	4.3	0.0
TROSKO	09.00	10.95	55.5	-002.0	19.0	1900.5-71.5	7.0	2.5	7.4
TSUMBI	-19.22	17.70	-5.9	-00.0	03.0	1904.0-75.5	4.3	2.4	3.4
TUCSON	32.25	-110.03	-110.1	-07.1	107.1	1900.5-77.5	7.5	3.7	0.7
UJLEN	00.10	-109.04	-104.0	25.1	-117.4	1900.5-70.5	0.1	12.2	12.2
ULAN BATOR	47.05	107.05	-09.2	-17.3	-05.2	1900.5-75.5	4.2	1.4	0.2
VALENTIA	51.03	-10.25	110.3	-50.1	25.4	1900.5-70.5	4.7	9.3	0.3
VANNOVSKAYA	37.95	50.11	171.5	53.4	50.0	1900.5-74.5	0.7	5.5	12.4
VASSOURAS	-22.40	-43.05	44.5	-120.5	-71.9	1900.5-73.5	0.3	3.0	3.3
VICTORIA	40.52	-123.42	-17.0	-0.0	-320.2	1900.5-70.5	5.3	0.3	7.1
VOSTOK	-70.45	100.07	-17.9	129.0	111.0	1900.5-70.5	20.4	14.2	10.0
VOYEVKOV	50.99	30.70	04.0	23.2	-201.0	1900.5-70.5	5.9	10.2	0.2
VYSOKAY DUBHAVA	50.73	01.07	-291.0	-123.5	-521.0	1900.5-00.5	2.3	1.3	1.4
	50.73	01.07	-297.5	-112.0	-402.0	1907.5-70.5	3.1	1.7	4.2
WILKES	-00.25	110.50	019.2	-290.5	29.4	1900.5-00.5	7.7	3.3	5.3
WINGST	53.74	9.07	44.4	40.1	-54.7	1900.5-70.5	0.0	0.0	3.0
YAKUTSK	02.02	129.72	40.5	-110.3	113.7	1900.5-75.5	4.7	0.2	13.2
YANGI-BAZAR	41.33	09.02	-301.0	01.0	-40.3	1904.5-70.5	0.1	4.7	13.4
YUZHO SAKHALSK	40.95	142.72	30.0	-105.0	-151.3	1900.5-09.5	4.0	3.7	5.2
	40.95	142.72	-04.3	-48.7	110.0	1970.5-70.5	1.0	0.0	1.0
ZAVRESHNE	55.03	40.05	-194.5	-115.7	-240.2	1900.0-77.0	3.5	2.3	2.7

observatory surface data in the solution in a consistent manner, techniques were used to remove the major parts of the crustal contributions. From the available scalar marine data over the years 1970-1974, 39 long, straight tracks of length greater than 1200 km were selected. A low pass filter was applied to each track, removing anomaly wavelengths shorter than 500 km. Approximately 300 measurements were then taken along the filtered tracks. A measurement standard deviation of 10 nT was used in weighting the data in the solution, although analysis of crossing points for the 39 tracks indicated differences on the order of 50 nT when corrected for secular variation. The higher weighting reflects our regard for the relative importance of these data in an area devoid of other surface observations. Approximately 600 measurements from 150 repeat stations were utilized to fill sparse data regions in Central and South America, Africa and Australia. Only stations with three or more occupations and good data quality were accepted. As there were generally insufficient data available for the repeat stations to solve for independent anomaly bias vectors, quadratic polynomial fits to these data were time differentiated to remove the assumed constant crustal influence. Measurement standard deviations for the "differentiated" repeat data were arrived at by utilizing the "differentiated" value, together with observatory and marine data, to derive a degree/order eight model. The standard deviations to that model were 0.2 deg/year for $\dot{\rho}$ and $\dot{\lambda}$ and 5 nT/year for \dot{H} , \dot{Z} and \dot{B} , taken collectively. These were adopted as measurement standard deviations for the repeat station data in the present analysis.

RESULTS

In order to test the usefulness of solving for anomalies at the observatories and of including second and third time derivatives, a model not incorporating MAGSAT data was developed and its prediction capability tested by comparing it to the MGST(6/80) model based only on MAGSAT

data. The test model, denoted PMAG(7/80), as well as the final model, denoted GSFC(9/80), was of degree/order 13 in its constant and first derivative terms, of degree/order six in its second derivative terms and of degree/order four in its third derivative terms. Table 4a gives the coefficient values and their first derivatives (secular variation), and Table 4b the second and third derivatives, for the GSFC(9/80) model. The standard error is given in parenthesis beside each coefficient. This is to be used as an error estimate only with caution because its accuracy depends upon (1) the accuracy of the σ_1 used to weight the data (and the validity of the assumptions that the data are uncorrelated and have gaussian error) and (2) the validity (accuracy and completeness) of our model. In practice the standard errors tend to underestimate the actual error but are nonetheless useful as an indication of the magnitude of error in each coefficient and of the relative accuracies between coefficients.

Table 5 summarizes a statistical evaluation of these models and two other recent (pre-MAGSAT) models. Model AWC75 (secular variation part) was derived by Peddie and Fabiano (1976) using data from 1967 through 1974 and model WC80 was derived by Barker et al (1981) using data from 1950 through 1980, but their secular variation model is thought to be applicable mainly from 1974-1977. AWC75 and WC80 include constant terms through degree/order 12 and first time derivatives through degree/order eight. In Table 5 MGST(6/80) is included as a standard of comparison for the 1980 epoch. Of the pre-MAGSAT models it is seen that PMAG(7/80) is the best predictive model. This indicates that, at least over a three-year interval, its temporal derivatives are not wildly varying beyond the data span. It should be noted that a similar model which did not include the observatory anomaly solution performed badly when used as a predictor, i.e. the presence of the anomaly solution affects the solution for the temporal terms in a positive way. The GSFC(9/80) model represents the 1980 field well because it incorporates MAGSAT data. It is, however, slightly deteriorated from MGST(6/80). This

ORIGINAL PAGE IS
OF POOR QUALITY

Table 4a

OSPC (1968) MAGNETIC FIELD MODEL
MEAN RADIUS OF THE EARTH IS 6371.2 KM; MEAN EPOCH IS 1968.0

r	θ	δ_r^m	δ_θ^m	δ_ϕ^m	δ_ψ^m
1	0	-3987.9 (0.0)		39.81 (0.10)	
1	1	-1057.4 (0.0)	9992.7 (1.0)	9.00 (0.10)	-9.04 (0.21)
2	0	-1058.7 (0.0)		-10.83 (0.14)	
2	1	2027.7 (0.0)	-2192.0 (0.0)	4.70 (0.13)	-10.74 (0.10)
2	2	1002.0 (1.0)	-1002.0 (1.1)	9.00 (0.10)	-20.82 (0.10)
3	0	1200.2 (0.4)		4.81 (0.12)	
3	1	-2100.0 (0.0)	-200.5 (0.0)	-3.00 (0.12)	-0.57 (0.13)
3	2	1201.3 (0.0)	270.0 (0.0)	-2.10 (0.12)	1.04 (0.13)
3	3	800.0 (1.0)	-201.0 (1.0)	3.07 (0.10)	-0.02 (0.10)
4	0	607.1 (0.3)		-2.30 (0.10)	
4	1	700.2 (0.4)	211.0 (0.4)	-2.34 (0.09)	3.00 (0.10)
4	2	207.2 (0.0)	-200.0 (0.0)	-10.00 (0.10)	1.00 (0.10)
4	3	-410.0 (0.4)	02.4 (0.4)	-3.02 (0.11)	0.77 (0.10)
4	4	100.0 (0.0)	-200.0 (1.0)	-0.04 (0.12)	-2.73 (0.13)
5	0	-217.1 (0.2)		-1.04 (0.04)	
5	1	207.0 (0.2)	00.2 (0.2)	-0.00 (0.04)	3.20 (0.04)
5	2	201.0 (0.2)	100.0 (0.2)	-0.73 (0.04)	0.00 (0.04)
5	3	-74.2 (0.4)	-100.7 (0.4)	-0.81 (0.06)	-0.02 (0.06)
5	4	-101.0 (0.2)	-77.7 (0.2)	0.11 (0.00)	1.00 (0.00)
5	5	-07.7 (0.7)	01.0 (0.0)	1.00 (0.07)	0.07 (0.07)
6	0	00.1 (0.2)		0.70 (0.03)	
6	1	00.0 (0.2)	-14.0 (0.2)	-0.04 (0.03)	0.03 (0.03)
6	2	02.0 (0.2)	03.4 (0.2)	3.00 (0.04)	-1.20 (0.03)
6	3	-101.4 (0.2)	70.0 (0.2)	2.20 (0.04)	-0.00 (0.04)
6	4	3.0 (0.2)	-02.0 (0.2)	0.44 (0.04)	0.11 (0.04)
6	5	14.1 (0.4)	-1.0 (0.2)	1.70 (0.04)	0.00 (0.04)
6	6	-107.1 (0.0)	17.0 (0.0)	1.34 (0.00)	2.72 (0.07)
7	0	71.0 (0.1)		0.00 (0.01)	
7	1	-00.1 (0.1)	-03.2 (0.1)	-0.20 (0.01)	-1.44 (0.01)
7	2	1.3 (0.1)	-27.1 (0.1)	0.00 (0.01)	-0.03 (0.01)
7	3	20.1 (0.2)	-0.0 (0.2)	0.00 (0.01)	0.10 (0.01)
7	4	-13.0 (0.2)	10.0 (0.2)	0.04 (0.01)	0.00 (0.01)
7	5	0.0 (0.2)	17.0 (0.2)	0.17 (0.02)	-0.37 (0.02)
7	6	10.0 (0.2)	-23.0 (0.2)	-0.20 (0.01)	0.00 (0.02)
7	7	-2.7 (0.0)	-0.0 (0.7)	0.00 (0.04)	0.04 (0.04)
8	0	10.0 (0.1)		0.00 (0.01)	
8	1	7.2 (0.1)	7.0 (0.1)	0.00 (0.01)	-0.00 (0.01)
8	2	0.0 (0.1)	-17.7 (0.1)	0.22 (0.01)	-0.30 (0.01)
8	3	-10.4 (0.1)	3.2 (0.1)	0.00 (0.01)	-0.00 (0.01)
8	4	-7.1 (0.2)	-22.4 (0.2)	-0.24 (0.01)	-0.34 (0.01)
8	5	4.0 (0.2)	9.4 (0.2)	-0.30 (0.01)	0.31 (0.01)
8	6	3.7 (0.2)	10.3 (0.2)	0.03 (0.02)	-0.04 (0.02)
8	7	7.1 (0.2)	-13.4 (0.2)	-0.40 (0.02)	-0.07 (0.01)
8	8	-1.3 (0.7)	-10.2 (0.7)	-0.20 (0.03)	0.00 (0.04)
9	0	0.2 (0.1)		-0.31 (0.01)	
9	1	10.7 (0.1)	-21.0 (0.1)	0.17 (0.01)	0.00 (0.01)
9	2	1.0 (0.1)	10.0 (0.1)	-0.04 (0.01)	0.00 (0.01)
9	3	-12.0 (0.1)	0.0 (0.1)	0.02 (0.01)	0.24 (0.01)
9	4	0.2 (0.1)	-4.0 (0.1)	-0.12 (0.01)	-0.10 (0.01)
9	5	-3.0 (0.1)	-7.0 (0.1)	-0.27 (0.01)	-0.27 (0.01)
9	6	-1.1 (0.2)	0.0 (0.2)	-0.04 (0.01)	-0.02 (0.01)
9	7	7.1 (0.2)	10.0 (0.2)	0.27 (0.01)	-0.00 (0.01)
9	8	1.0 (0.2)	-5.0 (0.2)	-0.00 (0.01)	-0.20 (0.01)
9	9	-0.0 (0.0)	2.1 (0.0)	-0.40 (0.03)	0.10 (0.03)
10	0	-3.0 (0.1)		-0.12 (0.01)	
10	1	-4.1 (0.1)	1.0 (0.1)	-0.00 (0.01)	-0.07 (0.01)
10	2	2.7 (0.1)	-0.1 (0.1)	0.04 (0.01)	-0.00 (0.01)
10	3	-0.0 (0.1)	2.0 (0.1)	-0.00 (0.01)	0.00 (0.01)
10	4	-1.0 (0.1)	0.0 (0.1)	0.01 (0.01)	-0.00 (0.01)
10	5	0.2 (0.1)	-4.0 (0.1)	0.01 (0.01)	-0.01 (0.01)
10	6	2.0 (0.1)	-1.0 (0.1)	-0.10 (0.01)	-0.14 (0.01)
10	7	1.3 (0.2)	-1.1 (0.2)	0.10 (0.01)	0.12 (0.01)
10	8	2.4 (0.2)	4.4 (0.2)	0.07 (0.01)	0.14 (0.01)
10	9	3.2 (0.2)	-0.0 (0.2)	0.00 (0.01)	-0.00 (0.01)
10	10	-0.3 (0.0)	-0.2 (0.0)	0.03 (0.02)	-0.00 (0.03)
11	0	2.3 (0.1)		-0.02 (0.01)	
11	1	-0.0 (0.1)	1.1 (0.1)	0.03 (0.01)	-0.03 (0.01)
11	2	-2.3 (0.1)	2.4 (0.1)	-0.03 (0.01)	-0.04 (0.01)
11	3	2.1 (0.1)	-2.1 (0.1)	-0.13 (0.01)	-0.02 (0.01)
11	4	0.3 (0.1)	-2.3 (0.1)	0.00 (0.01)	0.00 (0.01)
11	5	-0.4 (0.1)	0.4 (0.1)	-0.02 (0.01)	-0.02 (0.01)
11	6	-0.0 (0.1)	-0.1 (0.1)	-0.01 (0.01)	0.02 (0.01)
11	7	1.4 (0.1)	-3.0 (0.1)	-0.01 (0.01)	-0.10 (0.01)
11	8	1.0 (0.1)	-0.2 (0.2)	-0.11 (0.01)	0.00 (0.01)
11	9	-0.0 (0.2)	-0.7 (0.2)	0.00 (0.01)	0.10 (0.01)
11	10	1.0 (0.2)	-1.7 (0.2)	-0.10 (0.01)	-0.00 (0.01)
11	11	3.4 (0.4)	-0.1 (0.4)	0.00 (0.02)	-0.20 (0.02)
12	0	-2.0 (0.1)		-0.04 (0.01)	
12	1	-0.2 (0.1)	0.0 (0.1)	-0.03 (0.01)	0.00 (0.01)
12	2	0.0 (0.1)	0.0 (0.1)	0.11 (0.01)	-0.00 (0.01)
12	3	-0.3 (0.1)	2.0 (0.1)	-0.02 (0.01)	0.00 (0.01)
12	4	-0.2 (0.1)	-1.0 (0.1)	-0.00 (0.01)	-0.13 (0.01)
12	5	1.1 (0.1)	0.0 (0.1)	0.04 (0.01)	0.04 (0.01)
12	6	-0.3 (0.1)	0.2 (0.1)	0.03 (0.01)	-0.00 (0.01)
12	7	0.1 (0.1)	0.2 (0.1)	0.04 (0.01)	0.03 (0.01)
12	8	0.2 (0.1)	-0.3 (0.1)	0.01 (0.01)	-0.10 (0.01)
12	9	-0.0 (0.1)	-0.0 (0.1)	-0.00 (0.01)	-0.00 (0.01)
12	10	0.0 (0.2)	-0.0 (0.2)	0.01 (0.01)	0.00 (0.01)
12	11	0.0 (0.2)	0.0 (0.2)	0.00 (0.01)	-0.07 (0.01)
12	12	0.3 (0.2)	-0.1 (0.2)	-0.03 (0.02)	-0.01 (0.02)
13	0	0.0 (0.1)		0.02 (0.01)	
13	1	-0.2 (0.1)	0.3 (0.1)	0.03 (0.01)	0.07 (0.01)
13	2	0.2 (0.1)	0.2 (0.1)	-0.00 (0.01)	-0.01 (0.01)
13	3	-0.0 (0.1)	1.0 (0.1)	-0.00 (0.01)	0.03 (0.01)
13	4	0.2 (0.1)	0.0 (0.1)	-0.00 (0.01)	0.00 (0.01)
13	5	0.0 (0.1)	-1.0 (0.1)	0.01 (0.01)	-0.00 (0.01)
13	6	0.2 (0.1)	0.2 (0.1)	0.03 (0.01)	0.00 (0.01)
13	7	0.3 (0.1)	1.2 (0.1)	0.03 (0.01)	0.00 (0.01)
13	8	-0.0 (0.1)	-0.2 (0.1)	0.00 (0.01)	-0.01 (0.01)
13	9	0.2 (0.1)	0.7 (0.1)	-0.01 (0.01)	0.01 (0.01)
13	10	-0.4 (0.1)	-0.1 (0.1)	0.00 (0.01)	-0.02 (0.01)
13	11	0.2 (0.2)	-0.0 (0.2)	0.02 (0.01)	-0.04 (0.01)
13	12	-0.0 (0.2)	0.4 (0.2)	0.00 (0.01)	0.00 (0.01)
13	13	0.0 (0.3)	-0.4 (0.3)	0.07 (0.02)	-0.01 (0.02)

Table 4b

GSFC (9/80) MAGNETIC FIELD MODEL
(MEAN RADIUS OF THE EARTH IS 6371.2 KM; MEAN EPOCH IS 1980.0)
(CONTINUED)

n	m	g_n^m	h_n^m	g_n^m	h_n^m	g_n^m	h_n^m
1	0	-0.815 (0.032)				-0.0906 (0.0027)	
1	1	-0.449 (0.041)	1.158 (0.046)			-0.0498 (0.0041)	0.1914 (0.0046)
2	0	0.588 (0.026)				0.0384 (0.0023)	
2	1	0.497 (0.026)	-2.890 (0.030)			0.0264 (0.0023)	-0.2874 (0.0026)
2	2	0.694 (0.037)	-1.215 (0.041)			0.0198 (0.0039)	-0.0804 (0.0042)
3	0	1.304 (0.023)				0.1140 (0.0020)	
3	1	1.337 (0.024)	-2.218 (0.026)			0.1134 (0.0022)	-0.1836 (0.0024)
3	2	0.352 (0.024)	-0.156 (0.026)			0.0634 (0.0022)	-0.0168 (0.0023)
3	3	1.147 (0.034)	-0.489 (0.033)			0.0840 (0.0034)	-0.0690 (0.0033)
4	0	-0.248 (0.019)				-0.0240 (0.0017)	
4	1	-0.085 (0.018)	-0.240 (0.021)			-0.0012 (0.0016)	-0.0366 (0.0018)
4	2	-0.806 (0.020)	0.067 (0.021)			-0.0504 (0.0019)	0.0090 (0.0020)
4	3	-0.284 (0.021)	1.108 (0.021)			-0.0064 (0.0019)	0.1092 (0.0019)
4	4	-0.448 (0.026)	-0.192 (0.026)			-0.0354 (0.0026)	-0.0186 (0.0030)
5	0	-0.160 (0.003)					
5	1	-0.096 (0.003)	0.173 (0.003)				
5	2	-0.198 (0.003)	-0.135 (0.003)				
5	3	-0.272 (0.004)	0.107 (0.004)				
5	4	0.031 (0.004)	-0.035 (0.004)				
5	5	0.019 (0.006)	0.018 (0.006)				
6	0	0.077 (0.002)					
6	1	-0.063 (0.002)	0.048 (0.003)				
6	2	0.156 (0.003)	-0.074 (0.003)				
6	3	-0.025 (0.003)	-0.135 (0.003)				
6	4	0.036 (0.003)	0.095 (0.003)				
6	5	0.078 (0.003)	0.005 (0.003)				
6	6	0.156 (0.005)	0.081 (0.006)				

ORIGINAL PAGE IS
OF POOR QUALITY

Table 5

DATA TYPE	STATISTIC TYPE	MODEL				
		MRST(6/80)	AMC75	WCM	PMAG(7/80)	GSFC(9/80)
Magsat scalar	r.m.s.	8.2	138.9	118.7	82.2	10.1*
	mean	0.1	60.0	-20.6	-24.0	-1.6
	std. dev.	8.2	125.2	116.9	78.8	10.0
X-component***	r.m.s.	7.6	100.1	91.7	65.5	9.0
	mean	-0.2	24.7	-33.4	-27.9	-1.4
	std. dev.	7.6	97.0	85.5	59.3	8.9
Y-component***	r.m.s.	7.4	79.6	59.7	62.7	8.5
	mean	0.1	-1.3	-1.1	-1.6	-0.1
	std. dev.	7.4	79.6	59.7	62.7	8.5
Z-component***	r.m.s.	6.9	157.4	113.2	98.3	9.2
	mean	-2.5	24.9	20.9	3.1	-2.6
	std. dev.	6.5	155.4	111.3	97.2	9.2
P060 scalar	r.m.s.	--	60.8	121.6	6.7	6.0
	mean	--	43.8	21.3	0.0	-0.15
	std. dev.	--	54.4	119.8	6.7	6.9
Observatory X-component	r.m.s.	--	[1967-1974] 284.5	[1974-1977] 302.7	[1960-1977] 37.7**	[1960-1977] 39.9**
	mean	--	-24.7	41.5	3.5	5.6
	std. dev.	--	283.4	299.9	37.6	39.6
Y-component	r.m.s.	--	352.8	240.9	18.7	19.3
	mean	--	-48.3	-15.8	-0.06	0.4
	std. dev.	--	349.5	240.5	18.7	19.3
Z-component	r.m.s.	--	515.6	584.3	16.5	15.2
	mean	--	-23.7	-71.0	-0.05	-0.11
	std. dev.	--	515.0	579.9	16.5	15.2

*Magsat residuals to GSFC(9/80) were taken including the MRST(6/80) external terms with GSFC(9/80) because the Magsat data used to derive GSFC(9/80) was corrected for that external field.

**PMAG(7/80) and GSFC(9/80) include estimates of observatory "anomalies" which are taken into account when computing residuals.

***Does not include data at latitudes greater than 50° or less than -50°.

is not unexpected since it applies to a 20-year time period whereas MGST(6/80) is a direct fit to the two days of data involved.

Comparison with observatories shows typically high residuals for the models which do not estimate observatory anomalies (AWC75 and WC80). On the other hand, the observatory residuals for PMAG(7/80) and GSFC(9/80) are of the range one would expect from the published accuracy estimates of the observations, the internal consistency of the data from individual observatories, and the characteristics of unmodeled temporal variations. Note that no measurements with extreme residuals have been eliminated from this calculation, as is often done. This is because such extreme values are often due to the anomaly values solved for in PMAG(7/80) and GSFC(9/80) and so to compare the models all measurements should be utilized.

For further comparison, and to get a quantitative measure of the predictive capability of the models, statistics were computed of each model versus observatory data on a year-by-year basis. In doing so, we adopted the statistical measure used by Mead (1979) in a similar analysis, namely, half the width of the median 68% of the residual values. This is designated $\bar{\sigma}$, and would be equivalent to one standard error, σ , if the distribution were normal. The reason for adopting this measure is to avoid the situation where a few very large residuals dominate the statistics. Note that this is a different statistic than used in Table 5, and so the numbers are not directly comparable. In the plots to follow, some of the year-to-year changes in $\bar{\sigma}$ are due to a changing distribution of magnetic observatories. Figures 1-3 show the variation of $\bar{\sigma}$ with time for the X, Y, and Z components of observatory data relative to five field models: WC80, IGS75, AWC75, PMAG(7/80), and GSFC(9/80). IGS75 is the designation for the model derived by Barraclough et al (1975) from all available data from 1955 through about 1974. $\bar{\sigma}$ is rounded to the nearest 5 nT. The observatories used in this

evaluation are those listed in Table 3 (i.e. those used in deriving GSFC(9/80) and those listed in the Appendix. The statistic for GSFC(9/80) is computed without taking into account the local anomaly solution.

Examination of these plots shows that over its "lifetime" the GSFC(9/80) model describes the observatory data as well as or better than the other models. The deterioration of its representation prior to 1960 is also apparent. Of the models plotted, IGS75 has the longest useful "lifetime", presumably because the span of the data used to derive the model extended to the 1950's.

It is very apparent that these models, considered collectively, suffer from a data limitation such that a spherical harmonic analysis of reasonable degree/order cannot represent the data with a $\bar{\sigma}$ of better than about 100 nT in X, 90 nT in Y and 150 nT in Z. We attribute this to the presence of "crustal noise" in the data and believe that it is the fundamental limiting factor both on the accuracy of models based on such data and on our ability to evaluate model accuracy using such data.

A clearer picture of the model degradation is found in Figure 4. Here the statistics for GSFC(9/80) versus three components of observatory data are plotted taking into account the local anomaly solutions. The $\bar{\sigma}$ for each component is now in the 5 - 20 nT range from 1962.5 on. These values are commensurate with the accuracy of measurement at observatories; i.e., we believe we have very nearly eliminated the effect of crustal anomalies and that the statistic is now dominated by the actual measurement noise. Deterioration of the model begins at about 1961.5, within the data interval used by the model. This is attributed to the lack of satellite data, with their global coverage, prior to 1965. The amount of deterioration then increases rapidly outside the data interval. It is roughly doubled at 1958.5. Comparison of Figure 4

with Figures 1 - 3 indicates that the model deterioration becomes comparable to the "crustal noise" at about 1956. For many purposes this might be taken to be the useful limit of extrapolation of the model.

Figures 5 - 8 show the yearly averages at a series of observatories together with the field predicted by GSFC(9/80). Examination of these plots shows the need for the third time derivative, particularly for the X component at Alibag, Boulder, Gornotayezhnaya and Guam, and the Y and Z components at Gornotayezhnaya and Guam.

Figures 9 - 10 show data from two observatories not utilized in obtaining the solution. We have not, then, calculated the crustal component for these stations and none is included in the plots. This is most evident at Kodaikanal. Examination of Figures 9-10 shows that although the magnitude of the model differs from the data, the temporal change of the data is well represented throughout the 1960 - 1980 time period. Furthermore, the third time derivative is important for the Y components at Hurbanovo.

Figure 1

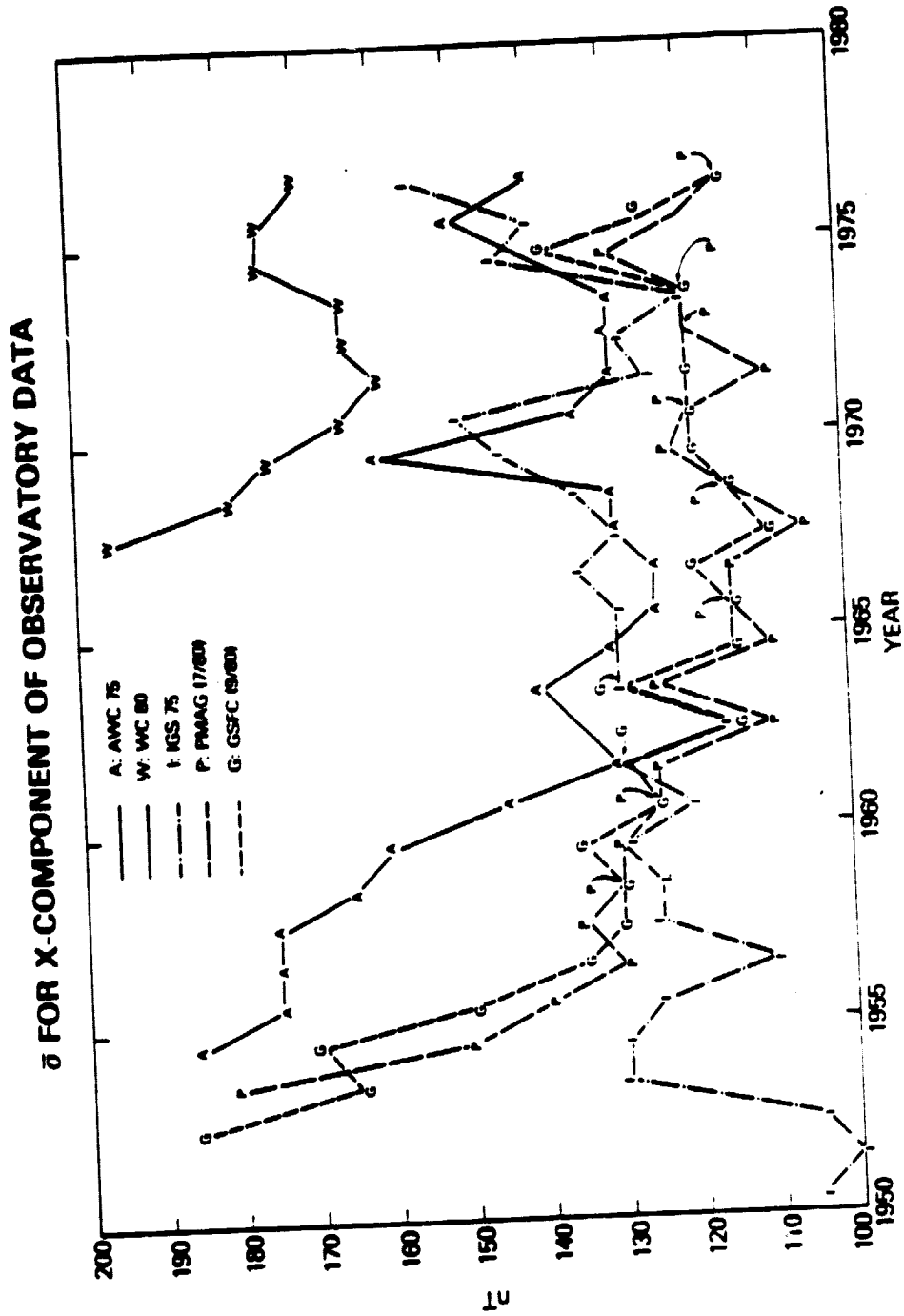


Figure 2

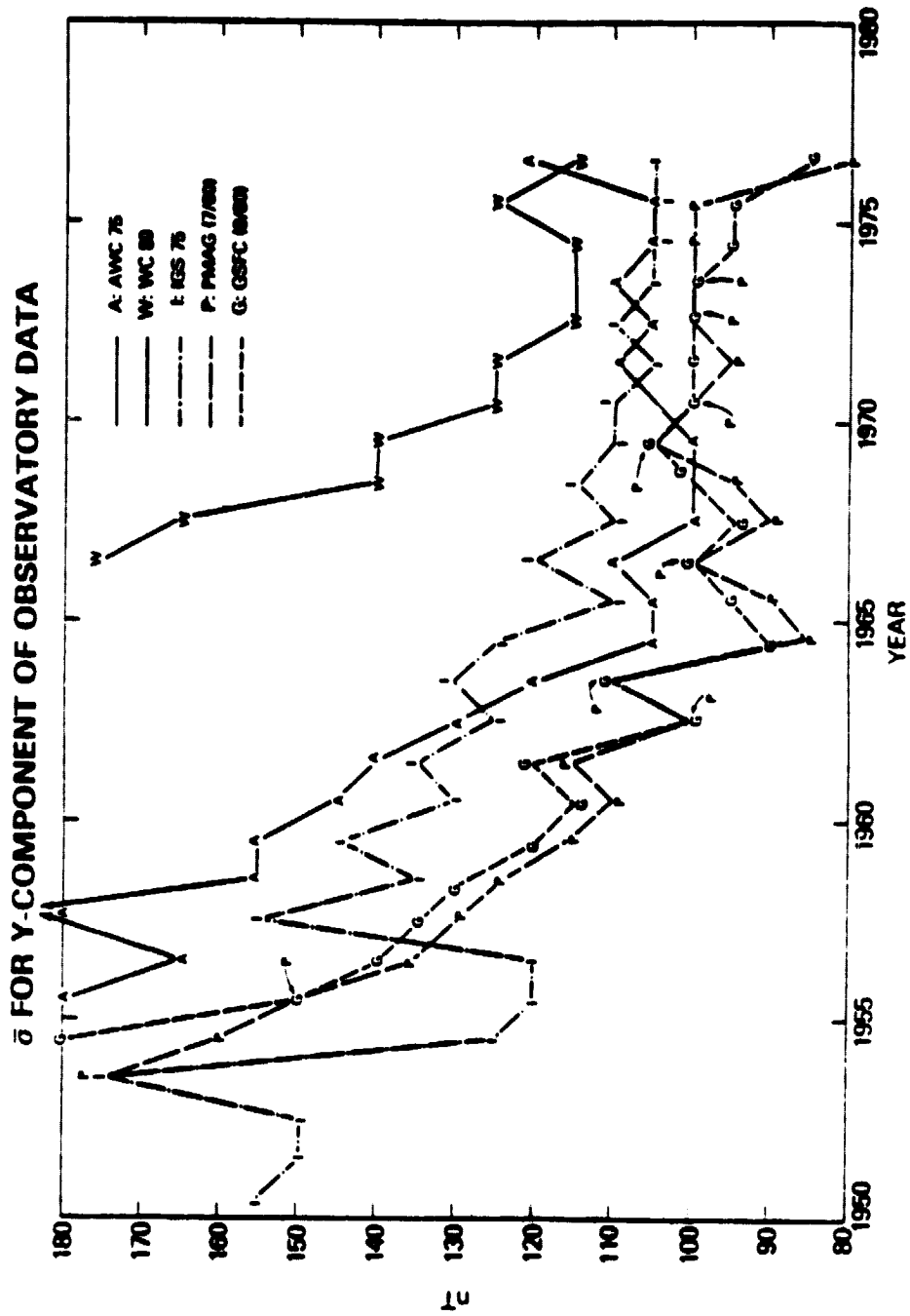


Figure 3

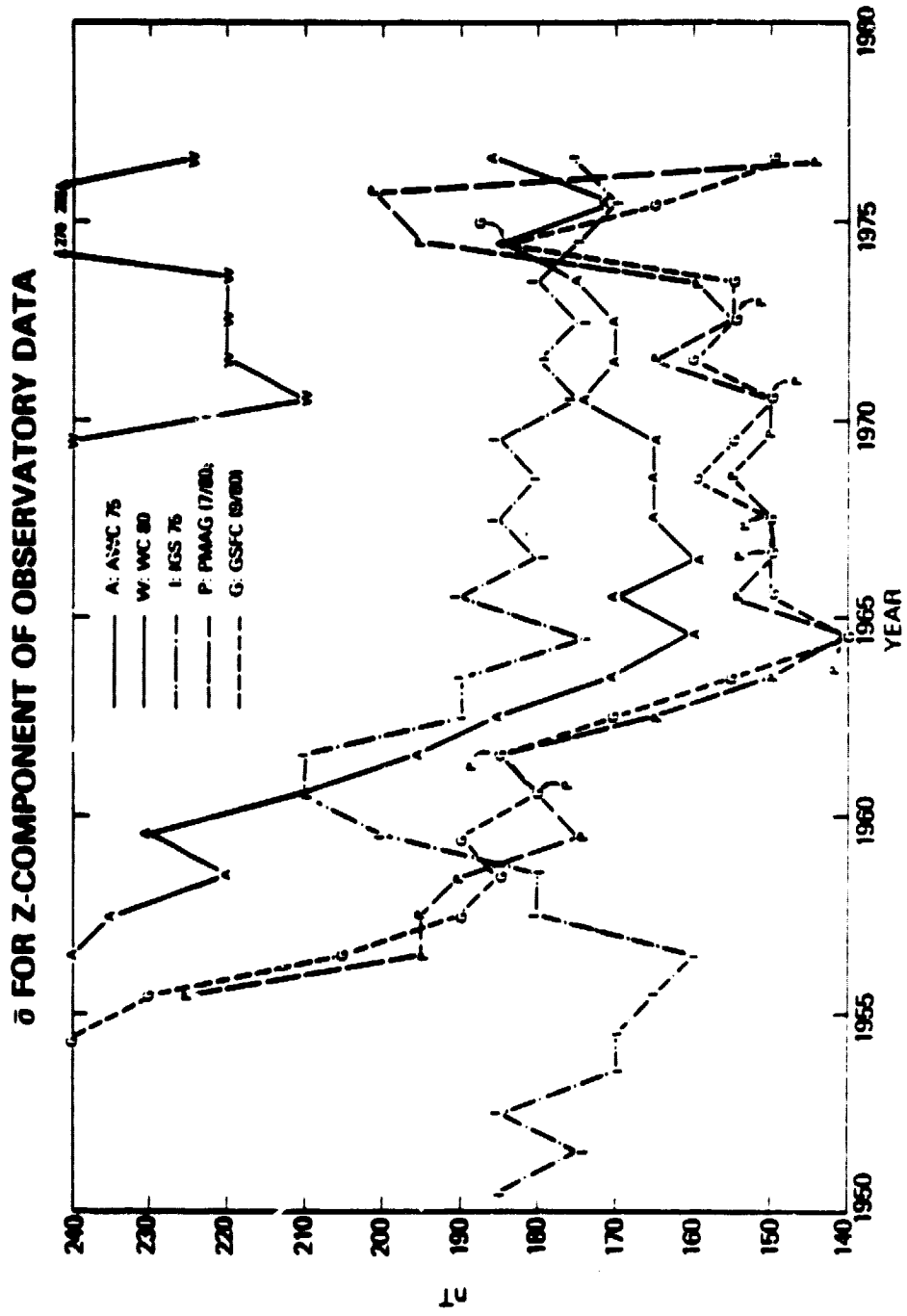


Figure 4

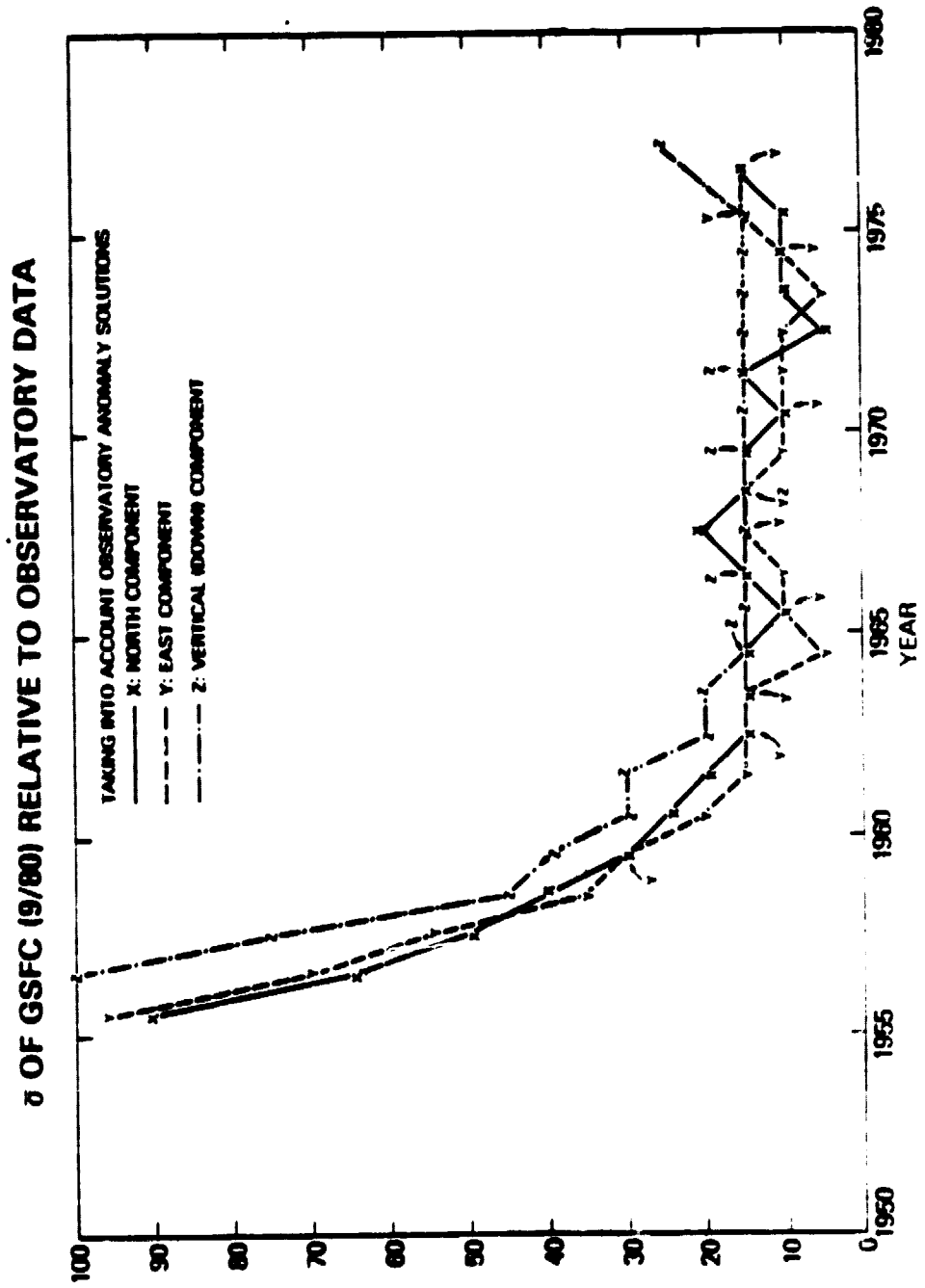


Figure 5

ALIBAG
LAT 13.64 LON 72.87 ALT 0.01 KM

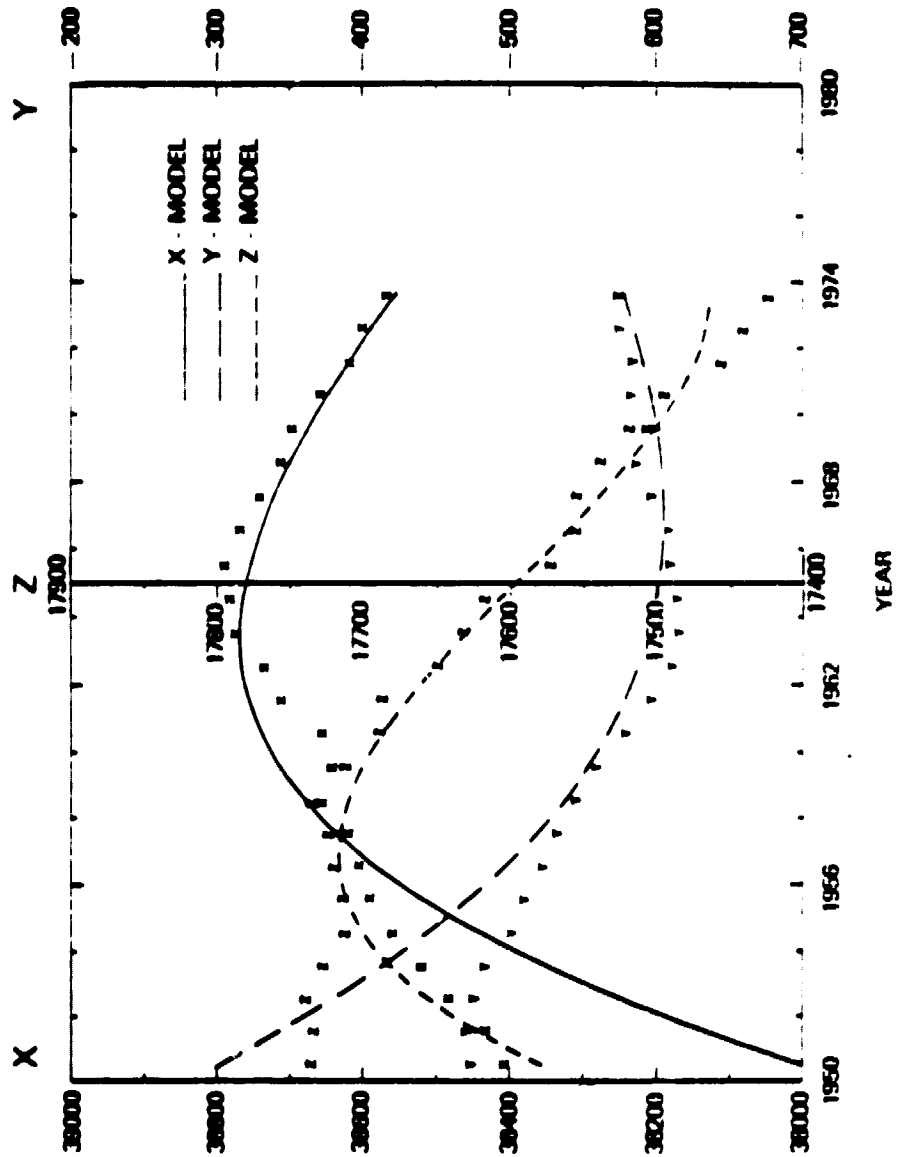


Figure 6

BOULDER
LAT 40.14 LON -105.24 ALT 1.65 KM

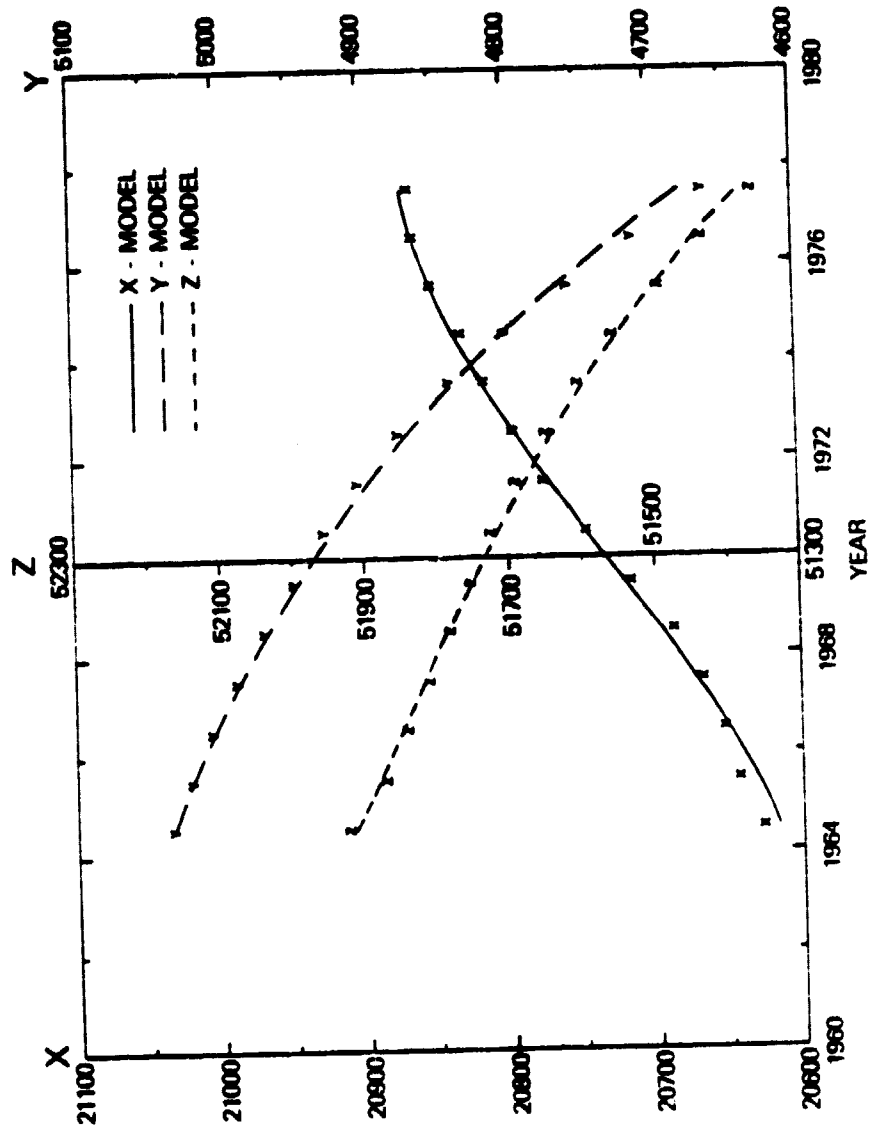


Figure 7

**GORNOTAYEZHNAYA
LAT 43.68 LON 132.17 ALT 0.30 KM**

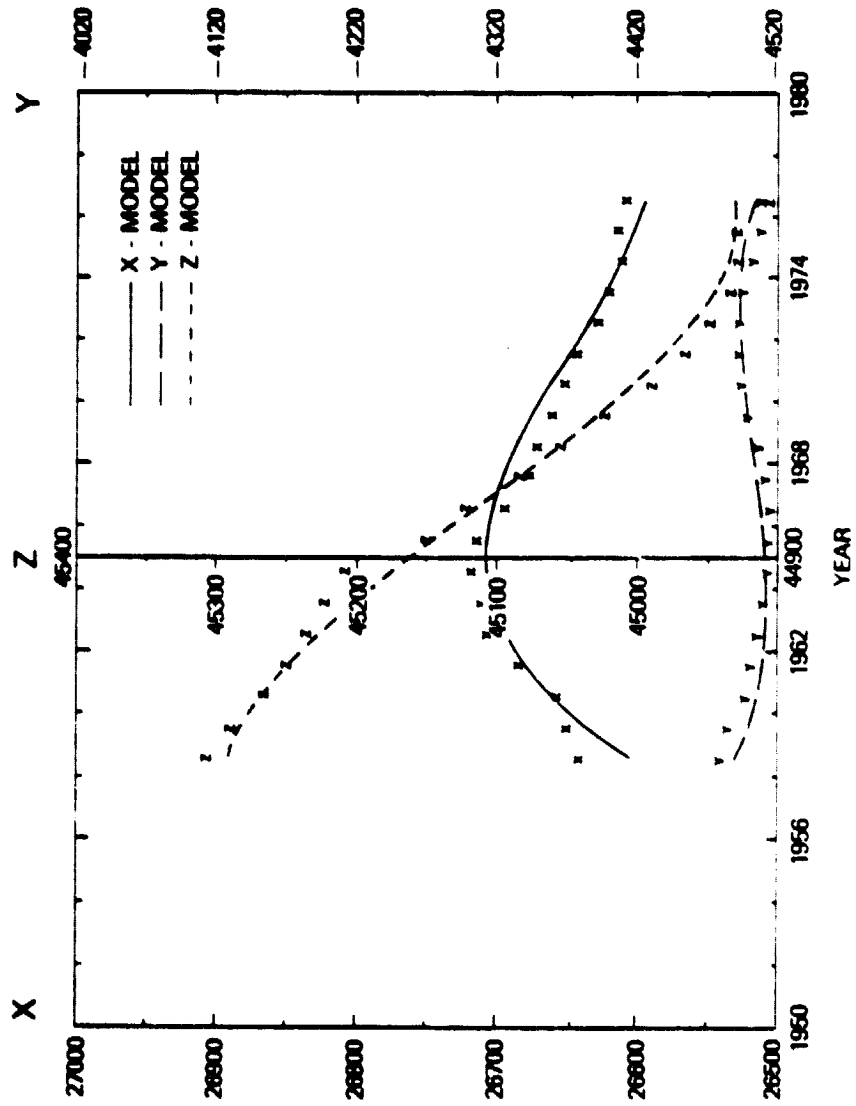


Figure 8

GUAM
LAT 13.58 LON 144.87 ALT 0.04 KM

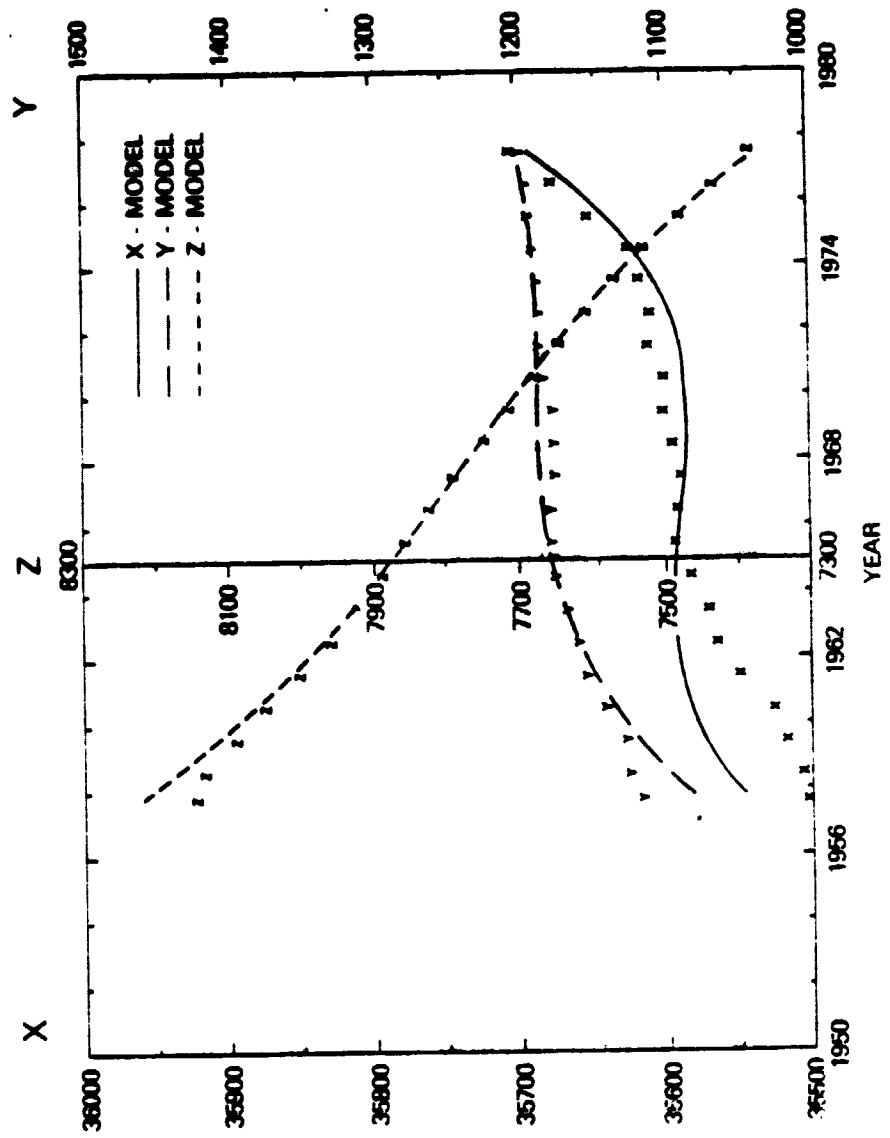


Figure 9

HURBANOVO
LAT 47.87 LON 18.19 ALT 0.12 KM

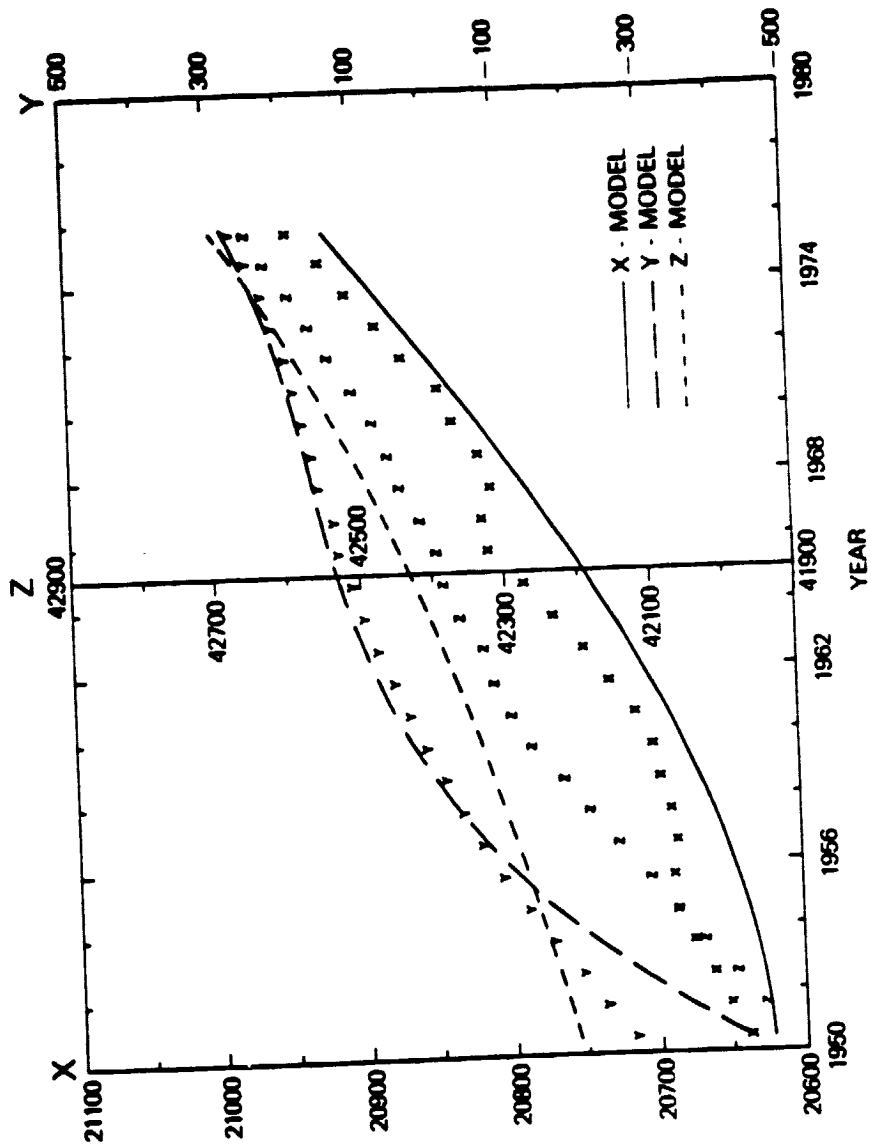
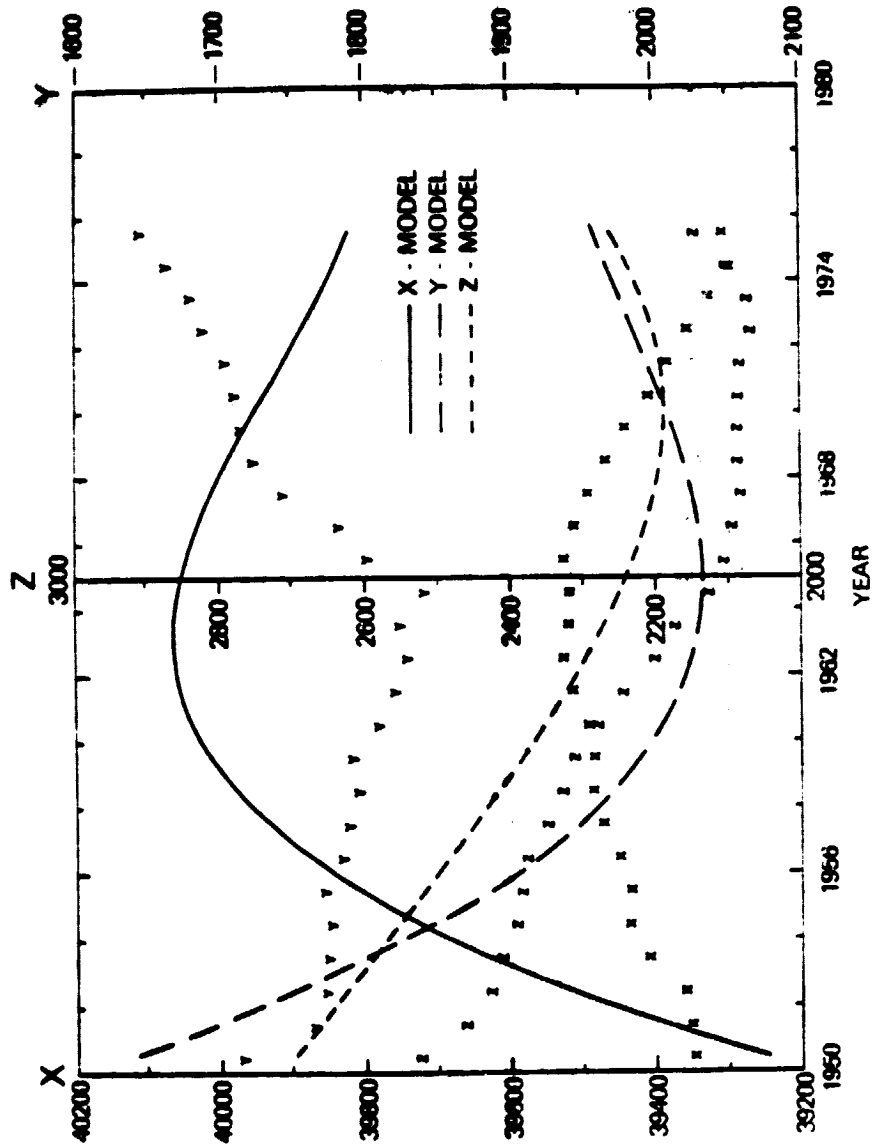


Figure 10

KODAIKANAL
LAT 10.23 LON 77.46 ALT 2.44 KM



DISCUSSION AND CONCLUSIONS

Observatory and other surface data are inadequate in space and time for determining accurate field models. Hints of the limitations of these data for defining the main field have repeatedly surfaced, as for example in the study already cited by Malin and Pocock (1969). Comparing Figure 1-3 with Figure 4 brings this limitation into clearer focus. The fact is that there is a "noise" with an "rms" ($\bar{\sigma}$) of about 100-150 nT in the observatory data set. We attribute this to the existence of crustal anomalies, although it is conceivable that error sources such as poor knowledge of data location, instrument inaccuracy or local magnetic contamination are contributing factors at some locations. Crustal anomalies are worldwide in distribution, have amplitude as high as several thousands of nT, and have a broad spectrum of spatial wavelengths. Because of the poor spatial distribution of surface data, any attempt to even partially model the anomaly field with such data will be plagued with aliasing problems. We conclude that these data alone provide sufficient accuracy only for models up to a degree and order of about eight. Satellite data are not immune to these limitations, although they are not as severe. Langel and Estes (1981) showed that crustal anomaly fields dominate the Magsat data for wavelengths shorter than those corresponding to degree and order fifteen. This means that with present methods of modeling, we cannot determine the main field representation beyond degree and order thirteen or fourteen, regardless of the quality of our data.

What must be appreciated is that the limitations of the data are limitations not only on modeling but also on the evaluation of models. For example, in considering Figure 1, the differences between models A, I, P and G between 1960 and 1975 are at the "noise" (anomaly) level of the observatory data and are not likely to be truly significant. To generalize this conclusion, a model derived from satellite data with accuracies of, say, 10-20 nT, cannot be accurately evaluated using observatory data unless the model is in error by several hundred nT.

The method of solving for observatory biases or anomalies presented here offers a partial solution to this data limitation. Further work is required to determine the dependence of the bias determination on other model parameters such as the time span involved, the degree and order of the constant and temporal terms, etc. One step in this direction has been taken in that we have determined the biases for several models of differing degree and order with only small changes in the values of the biases so determined.

Further such tests need to be performed. Moreover, it needs to be determined if the calculated biases are in reasonable accord with, say, aeromagnetic anomaly data. This is complicated by the fact that the untangling of the aeromagnetic anomalies from the main field model used to reduce the anomaly data is not straightforward.

Adequate representation and prediction of the temporal change of the earth's main field has, in our minds, not been achieved. In this paper, we have taken two steps which we believe improve the situation. First, we have included solution for the localized observatory anomaly fields and, second, we have utilized third time derivatives. The success of the second step depends upon inclusion of the first.

The use of second and third derivatives has certainly resulted in a model of good accuracy for a twenty year period. The advantages of this over the use of several individual models for a shorter period of time are continuity and that the highly accurate satellite data are allowed to provide some constraint at times remote from the data epoch and so, hopefully, increase the overall accuracy. Tests indicated that PMAG(7/80) predicted two to three years forward in time more accurately than other Pre-Magsat models. Comparison with observatory data (Figures 1-3, 5-10) indicates that GSFC(9/80) "predicts" (backward in time from 1960) within the 100-200 nT level for about four years. However, for

longer prediction, such models are clearly not suitable because the higher derivative terms begin to dominate and the resulting error increases at a more rapid rate than for models with, say, only first derivatives. A solution might be to taper the higher temporal derivatives to zero a few years beyond the existing data interval. This, however, is quite ad hoc and has little real justification. Another approach would be to continue to add temporal terms, including higher order derivatives, until, hopefully, some sort of convergence is achieved. From the discussion of Table 2, it is likely that higher degree and order second and third derivatives are significant. It is not clear, however, that temporal convergence will ever be achieved within any reasonable computer limitations or even that it is possible. The problem, of course, is that model constraints based on the physics of the core dynamo are not built into these models. In our view, until this is done it will not be possible to derive truly adequate "forecast" models.

ACKNOWLEDGMENTS

The authors wish to acknowledge the interesting discussions and contributions made by E. R. Lancaster of Goddard Space Flight Center in helping to develop some of the new modeling techniques presented in this paper.

Appendix: Observatories used for the statistics of Figures 1-3 but not included in the model solution are: Abinger, Abisko, Acacias, Aso, Averroes, Baguio, Bouzareah, Budakeszi, Budkov, Cambridge Bay, Castellaccio, Centro Geofisico, Cheltenham, Davao, Nehra Dun, Druzhnaya, Ebro, Eights, El Abiod Sidi, Elisabethville, Eskdalemuir, Gibilmanna, Gonzalez Videla, Hallett Station, Heard Island, Heiss Island, Helwan, Hollandia, Hurbanovo, Ibadan, Isla da Pascua, Jassy, Julianehaab II, Kanoya, Kanozan, Karavia, Katuura, Kiruna, Kodaikanal, Kuyper, L. America III, L. America V, Lazarevo, Luanda Golf, Manhay, Maputo, Marion Island, Mizusawa, Monte Capellino, Murmansk, Nagycenk, Nantes, Nitzanim, Norway Station, Novo-Kazalinsk, Orcadas del Sur, Patrick, Pendeli, Port-Alfred, Regensberg, Roi Baudouin, San Fernando, Simferopol, Srednikan, Stonyhurst, Surlari, Swider, Taipei, Tangerang, Thule I, Tikhaya Bay, Toledo, Tulsa, Voroshilov, Vykhodnoy, Watheroo, Wien Auhof, Wien Kobenzl, Witteveen, Yellowknife.

REFERENCES

Backus, G.E., Non-Uniqueness of the External Geomagnetic Field Determined by Surface Intensity Measurements, J. Geophys. Res., 75, 6337-6341, 1970.

Barker, F.S., D.R. Barraclough, and S.R.C. Malin, World Magnetic Charts for 1980 - Spherical Harmonic Models of the Geomagnetic Field and its Secular Variation, Geophys. J.R. Astr. Soc., in press, 1981.

Barraclough, D.R., J.M. Harwood, B.R. Leaton, and S.R.C. Malin, A Model of the Geomagnetic Field at Epoch 1975, Geophys. J. Royal Astr. Soc., 43, 645-659, 1975.

Barraclough, D.R., and S.R.C. Malin, Geomagnetic Secular Acceleration, Geophys. J.R. Astr. Soc., 58, 785-793, 1979.

Cain, J.C., S.J. Hendricks, R.A. Langel, and W.V. Hudson, A Proposed Model for the International Geomagnetic Reference Field - 1975, J. Geomagnet. Geoelec., Kyoto, 19, 335-355, 1967.

Hurwitz, L. and D.G. Knapp, Inherent Vector Discrepancies in Geomagnetic Main Field Models Based on Scalar F, J. Geophys. Res., 79, 3009-3013, 1974.

Langel, R.A., Near-Earth Magnetic Disturbance in Total Field at High Latitudes 1. Summary of Data from OGO 2, 4, and 6, J. Geophys. Res., 79, 2363-2371, 1974.

Langel, R.A. and R.H. Estes, A Geomagnetic Field Spectrum, submitted to Geophys. Res. Letters, 1982.

Langel, R.A., R.L. Coles, and M.A. Mayhew, Comparison of Magnetic Anomalies of Lithospheric Origin Measured by Satellite and Airborne Magnetometers over Western Canada, Can. J. Earth Sci., 17, 876-887, 1980a.

Langel, R.A., R.H. Estes, G.D., Mead, E.R. Fabiano and E.R. Lancaster, Initial Geomagnetic Field Model from Magsat Vector Data, Geophys. Res. Lett., 7, 793-796, 1980b.

Loves, F.J., Mean Square Values on the Sphere of Spherical Harmonic Vector Fields, J. Geophys. Res., 71, 2179, 1966.

Loves, F.J., Spatial Power Spectrum of the Main Geomagnetic Field, and Extrapolation to the Core, Geophys. J.R. Astr. Soc., 36, 717-730, 1974.

Malin, S.R.C. and S.B. Pockock, Geomagnetic Spherical Harmonic Analysis, Pure and Appl. Geophys., 75, 117-132, 1969.

Mead, G.D., An Evaluation of Recent Internal Field Models, in Quantitative Modeling of Magnetospheric Processes, W.P. Olson, Editor, Geophysical Monograph 21, 110-117, American Geophysical Union, 1979.

Peddie, N.W., and E.R. Fabiano, A Model of the Geomagnetic Field for 1975, J. Geophys. Res., 81, 2539-2542, 1976.

Stern, D.P. and J.H. Brückamp, Error Enhancement in Geomagnetic Models Derived from Scalar Data, J. Geophys. Res., 80, 1776-1782, 1975.

Stern, D.P., R.A. Langel and G.D. Mead, Backus Effect Observed by Magsat, Geophys. Res. Lett., 7, 941-944, 1980.

FIGURE CAPTIONS

- Figure 1: Variation of $\bar{\sigma}_x$ with time for observatory data relative to five field models, not including observatory anomalies.
- Figure 2: Variation of $\bar{\sigma}_y$ with time for observatory data relative to five field models, not including observatory anomalies.
- Figure 3: Variation of $\bar{\sigma}_z$ with time for observatory data relative to five field models, not including observatory anomalies.
- Figure 4: Variation of $\bar{\sigma}$ with time for GSFC(9/80), including observatory anomalies.
- Figure 5: Comparison of Alibag annual means (X,Y,Z) to values computed from GSFC(9/80), including the observatory anomaly. Data from this observatory was used in the solution for GSFC(9/80).
- Figure 6: Comparison of Boulder annual means (X,Y,Z) to values computed from GSFC(9/80), including the observatory anomaly. Data from this observatory was used in the solution for GSFC(9/80).
- Figure 7: Comparison of Gornotayezhnaya annual means (X,Y,Z) to values computed from GSFC(9/80), including the observatory anomaly. Data from this observatory was used in the solution for GSFC(9/80).

Figure 8: Comparison of Guam annual means (X,Y,Z) to values computed from GSFC(9/80), including the observatory anomaly. Data from this observatory was used in the solution for GSFC(9/80).

Figure 9: Comparison of Hurbanovo annual means (X,Y,Z) to values computed from GSFC(9/80). No observatory anomaly was computed because data from this observatory was not used in the solution for GSFC(9/80).

Figure 10: Comparison of Kodaikanal annual means (X,Y,Z) to values computed from GSFC(9/80). No observatory anomaly was computed because data from this observatory was not used in the solution for GSFC(9/80).